



HAL
open science

Proposition of a new qualification impact test for aerospace smart structures

Giulia Gastaldo, Younes Rafik, Marc Budinger, Valérie Pommier-Budinger,
Philippe Olivier, Pablo Navarro

► **To cite this version:**

Giulia Gastaldo, Younes Rafik, Marc Budinger, Valérie Pommier-Budinger, Philippe Olivier, et al..
Proposition of a new qualification impact test for aerospace smart structures. ICAS 2022 - 33rd
Congress of the International Council of the Aeronautical Sciences, Sep 2022, Stockholm, Sweden.
hal-03879795

HAL Id: hal-03879795

<https://hal.science/hal-03879795>

Submitted on 30 Nov 2022

HAL is a multi-disciplinary open access archive for the deposit and dissemination of scientific research documents, whether they are published or not. The documents may come from teaching and research institutions in France or abroad, or from public or private research centers.

L'archive ouverte pluridisciplinaire **HAL**, est destinée au dépôt et à la diffusion de documents scientifiques de niveau recherche, publiés ou non, émanant des établissements d'enseignement et de recherche français ou étrangers, des laboratoires publics ou privés.

PROPOSITION OF A NEW QUALIFICATION IMPACT TEST FOR AEROSPACE SMART STRUCTURES

Giulia Gastaldo¹, Younes Rafik², Marc Budinger², Valérie Pommier-Budinger¹, Philippe Olivier² & Pablo Navarro²

¹ISAE-SUPAERO, Université de Toulouse, Toulouse, 31055, France

²Institut Clément Ader (ICA), University of Toulouse, INSA, ISAE-SUPAERO, MINES ALBI, UPS, CNRS

Abstract

Piezoelectric materials are employed in several different aerospace applications thanks to their actuating and sensing abilities. They can be adopted to control vibration, stress distribution, aeroelastic stability, shape changes, and in structural health monitoring systems. Given the level of reliability required in aeronautics, it is of vital importance to ensure their correct functioning during all aircraft life and for critical events such as impacts. This paper proposes a novel test standard method to measure and qualify the damage resistance of smart PZT structures to a drop-weight impact event. Procedures for the quantification of damage through measurements of electromechanical characteristics are introduced and verified by impact tests.

Keywords: BVID, Smart structures, PZT, Impact

Nomenclature

BVID	Barely Visible Impact Damage
CAI	Compression After Impact
FEM	Finite Element Method
PZT	Lead Zirconate Titanate
SHM	Structural Health Monitoring

1. Introduction

Piezoelectric materials are widely employed in aerospace applications, thanks to their ability to behave both as actuator and as sensors. In the last decade, they have been studied for aircraft [1] [2], helicopter [3] and UAV [4] actuation applications, for electromechanical ice protection systems [5], as well as for structural health monitoring systems [6], [7], [8].

Despite the many benefits of adopting smart structures solutions, there are some critical aspects regarding piezoelectric transducers maintenance and functioning that must be taken into account. In fact, the deterioration or complete failure of the aforementioned transducers due to the external loading and environmental conditions negatively affect the performance of the system. Above all others, a threat to these embedded systems is the frequent occurrence of impact loads. When impact occurs, piezoelectric components may be subject to fracture, and this would lead to the degradation of their mechanical and electrical properties [9], [10]. Moreover, the adhesive bonding between the PZT sensors and the structure may be compromised as well, thus deteriorating the overall functioning of the system. Therefore, it is of utmost importance to ensure the integrity of piezoelectric components.

Many studies focus on the real-time failure detection. For the general evaluation of PZT structural conditions, Friswell and Inman introduced in [11] the concept of sensor validation for smart structures, which is the process of assessing the proper sensor functioning during operation. They were able to determine the functioning state of the sensors by comparing the subspace of the response and the one generated by the lower modes of the structure. Kershen et al. presented a sensor validation method based on the principal component analysis [12]. Another technique is based on the electromechanical impedance method firstly pioneered by Liang et al. [13] and Sun et al. [14] and then adopted for the detection of faulty sensors in structural health monitoring systems in the work proposed by Giurgiutiu et al. firstly in [15] and then in [16]. Park et al. proposed a sensor diagnostic process based on electrical admittance measurement [17]. They produced an impact in a composite plate, and they then evaluated the shift in the imaginary component of the measured admittance. In [18], Sun and Thong addressed the detection of debonding of piezoelectric actuators performing vibration control. The method is based on a control system which is sensitive to frequency changes due to the partial debonding of a PZT patch. Other changes can be measured to detect failures in piezoelectric patches. Wang et al. [19], [20] evaluated the changes on the dynamic piezoelectric constants to detect impact in a single PZT sensor. In [10] [21], the authors proposed a novel mechanism for characterizing smart structures using mechanical quality factor.

The approach developed in this article is different from real-time failure detection during operations. The proposed method aims to quantify the impact resistance of piezoelectric components before commissioning, in order to qualify and certify them for applications with high reliability requirements, such as aeronautical applications. This method is based on the current barely visible impact damage (BVID) test procedure combined with electromechanical characteristics measurements of smart structures. The novel procedure will be validated through experimental tests.

2. Extension of the BVID test for the qualification of smart structures

This section first recalls the BVID qualification test for composite laminates and then presents the proposed extension for the qualification of smart structures.

2.1 BVID test for the qualification of composite laminates

As previously mentioned, one sensitive aspect for aerospace structures is the occurrence of low-velocity impact events. This phenomenon has been thoroughly studied for composite laminates, as they suffer from important reduction in their mechanical properties when a localized damage is present in the structure. This type of damage is often caused by low-velocity impacts with objects, producing local indentation, delamination, or fiber/matrix cracking, which are hardly detectable under visual inspection. Barely visible impact damage (BVID) can have serious consequences on structural integrity, especially if the damage size grows under cyclic loading [22]. It mostly occurs in the form of local delamination, and it has a critical effect on the strength of composite materials. To evaluate the effect of barely visible impact damage on composites, one of the most used indicators adopted is the Compression After Impact (CAI) strength [23]. In fact, the CAI event can reduce the component's strength up to 60% in comparison to pristine samples [24], [25], [26], potentially leading to the complete failure of the structure. Given its great impact on the mechanical performance, the CAI strength is considered a critical design parameter which has to be evaluated in order to assess the tolerance to BVID in composite laminates.

For composite materials, the experimental studies are based on existing test methods and standards, such as the Airbus test method AITM 1–0010 [27] and the ASTM standard ASTM D7136 [28], which are specific for impact events. Once the impact tests have been carried out, the samples are further subject to compression after impact tests in accordance with ASTM D7137 [29] and CAI strengths are then evaluated.

2.2 BVID test for the qualification of piezoelectric smart structures: parameters and procedure

To enable the study of impact resistance of smart structures, it is necessary to adapt the test procedure and propose indicators significant of the operation of smart structures. In this paper, smart

structures under consideration are structures integrating electromechanical components and in particular piezoelectric transducers. Consequently, the indicators should be chosen for their ability to measure the electromechanical properties of smart structures.

First, let us analyze the electromechanical behavior of the smart structure. As it has been shown in previous articles by Pommier-Budinger et al. [30], [31], the performance of smart structures is linked to the value of the force factor characteristic of the electromechanical coupling. In case of piezoelectric materials, this parameter can be obtained from the electrical charges produced by a mechanical solicitation.

The reduced dynamical model of a resonant structure with one degree of freedom, thus having one piezoelectric actuator, can be written as:

$$\begin{cases} M\ddot{q} + D_s\dot{q} + Kq = NV \\ q_c = Nq + C_0V \end{cases} \quad (1)$$

The system of equations is constituted of a mechanical equation and an electrical equation. q is the modal displacement of the selected point for the reduced model, M the modal mass, K the modal stiffness, D_s the damping coefficient, N the force factor, q_c the electrical charge, V the voltage, and C_0 the blocked capacitance.

It is possible to compute [30] the force factor by calculating the electrical charge for a short circuit condition, $V = 0$ and using the second equation:

$$N = \frac{q_c}{q} \quad (2)$$

The evaluation of the force factor evolution is certainly the most interesting parameter for assessing the performance of smart structures. Indeed, in the case of actuation systems integrated in the structure, a decrease in this factor results in a loss of actuation capacities, such less effort or less displacement. In the case of sensors integrated in the structure, a decrease in the force factor induces a lower signal-to-noise ratio.

Second, let us consider the equivalent electric scheme of a piezoelectric transducer, as represented in figure 1. It is constituted by two different parallel branches: a static branch, which represents the purely electric behavior of the piezoelectric material, formed by the capacitance C_0 and the resistance R_0 , and a second motional branch, which is constituted by a resonant RLC circuit. C_0 is proportional to the surface of the transducer, so a decrease of C_0 can represent a part disconnected from the electrode due to a crack. The measurement of the turned-off capacitance C_0 is thus interesting since it is a good indicator of the structural health of the piezoelectric transducer.

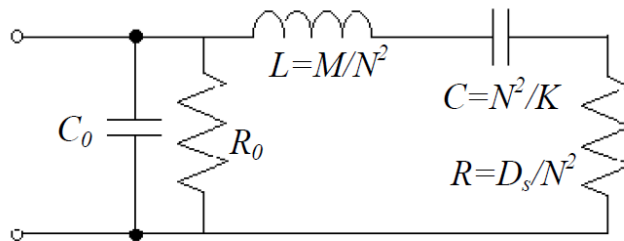


Figure 1 – Equivalent circuit [32]

Note: the parameter representing the dielectric losses within the piezoelectric transducer R_0 is assumed greater than the resistance of the motional branch R_s . Thus, R_0 will not be taken into account in the following sections.

To conclude, two characteristics of a smart piezoelectric structure interesting for quantifying its performance are the force factor and the turned-off capacitance. They will be considered as indicators of the structural integrity of the piezoelectric smart structure.

3. Measurement of performance indicators

The proposed method for the qualification of smart piezoelectric structures relies on an impact test and on the assessment of indicators which are representative of the performance of the smart structure. As explained in section 2, the objective is to evaluate two characteristic quantities obtained through non-destructive tests:

- the force factor N
- the turned-off electrical capacitance C_0

The testing procedure will be detailed in the following paragraphs.

3.1 Force factor (N)

The force factor is measured at the resonant frequency of the smart structure at a given mode. The sinusoidal supply voltage signal must be maintained until the steady state is reached.

From equation 2 deriving q_c and q with respect to time, it is possible to compute N using this formula:

$$N = \frac{I_m}{\dot{q}} \quad (3)$$

where I_m is the current going through the motional branch of the piezoelectric transducer and \dot{q} is the speed of a given point of the plate. For flexural modes, this point will be located on the plate surface, at an antinode of the selected mode. For an extensional mode, it will be located on one chosen edge of the plate.

The force factor N is different for every mode, and depends on the coupling of the piezoelectric transducer with the structure. This value is influenced by the location of the transducer and by the considered modal shape. The interest is to maximize N . For this purpose, if a flexural mode is considered, the piezoelectric transducer should be located at an antinode and the order of the mode should be selected to fulfill this condition. In our case, the PZT patch is located in the center of the plate, thus flexural symmetric modes are selected. On the contrary, for extensional modes, the PZT transducer should be located at a node of the mode shape.

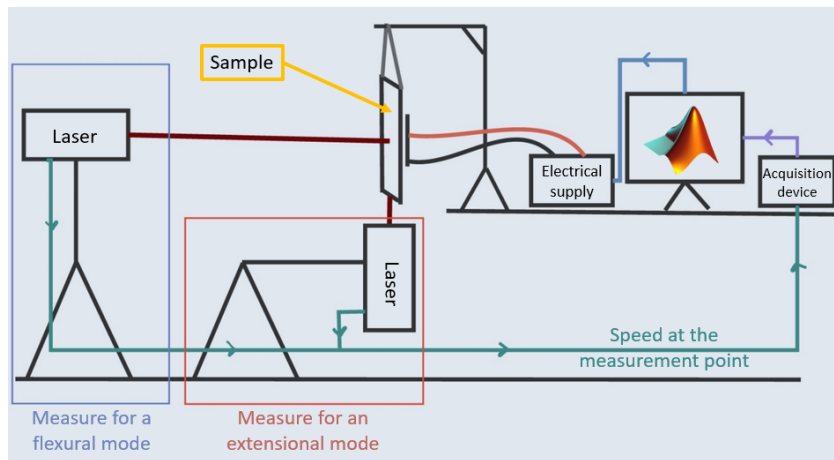


Figure 2 – Test setup

The setup to realize the measurements is presented in figure 2. The piezoelectric transducer is excited by a sinusoidal signal at the resonant frequency of the selected mode. The frequency can be

estimated using FEM models of the sample and determined precisely with a sweep around the estimated frequency. The speed at the maximum displacement of the mode is measured with the laser vibrometer positioned either to measure the displacement on the sample surface in case of flexural modes or the displacement on the sample edge in case of extensional modes. The motional current is measured using a power analyzer.

3.2 Electrical capacitance (C_0)

A method to estimate C_0 is to measure the electrical capacitance of the piezoelectric component at low frequency, far from the first resonant mode. Indeed, as shown in figure 3, the capacitance is almost constant at low frequencies. For this measurement, an impedance meter is used. At low frequencies, it is possible to measure the turned-off capacitance as:

$$C_0 = \lim_{\omega \rightarrow 0} \frac{Im(Y(\omega))}{\omega_s} \quad (4)$$

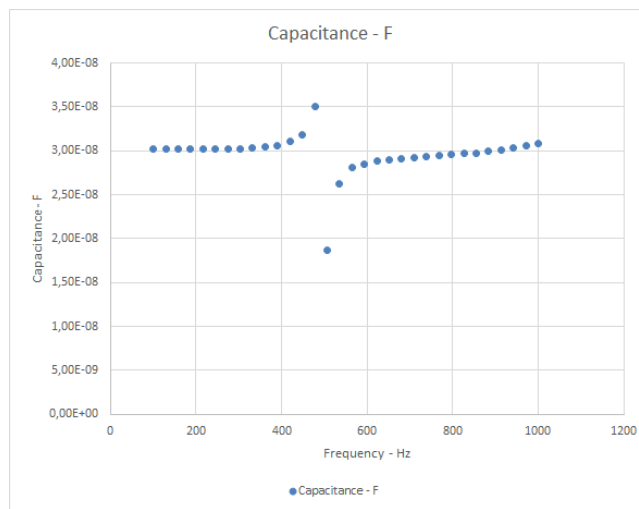


Figure 3 – Evolution of the capacitance according to the frequency

The setup for the measurement of C_0 is shown in figure 4. The piezoelectric transducer is plugged in the impedance meter and the plate is in free boundary condition.



Figure 4 – Setup for the measure of C_0

4. Test results

In this section, the procedure proposed for the qualification of the resistance to impact of piezoelectric structures is assessed. One set of samples is tested and the measurement of the indicators is carried out.

The objective is to realize measurements in order to verify the evolution of the indicators N and C_0 according to impact energy. Furthermore, the results obtained from the proposed procedure will be compared with the ones from conventional tests to assess the better suitability of this method to qualify smart structures.

4.1 Impact test

The impact tests are carried out according to AITM 1-0010 [27] and ASTM D7136 [28] standards. These correspond to the BVID standard, of which figure 5 gives a schematic representation.

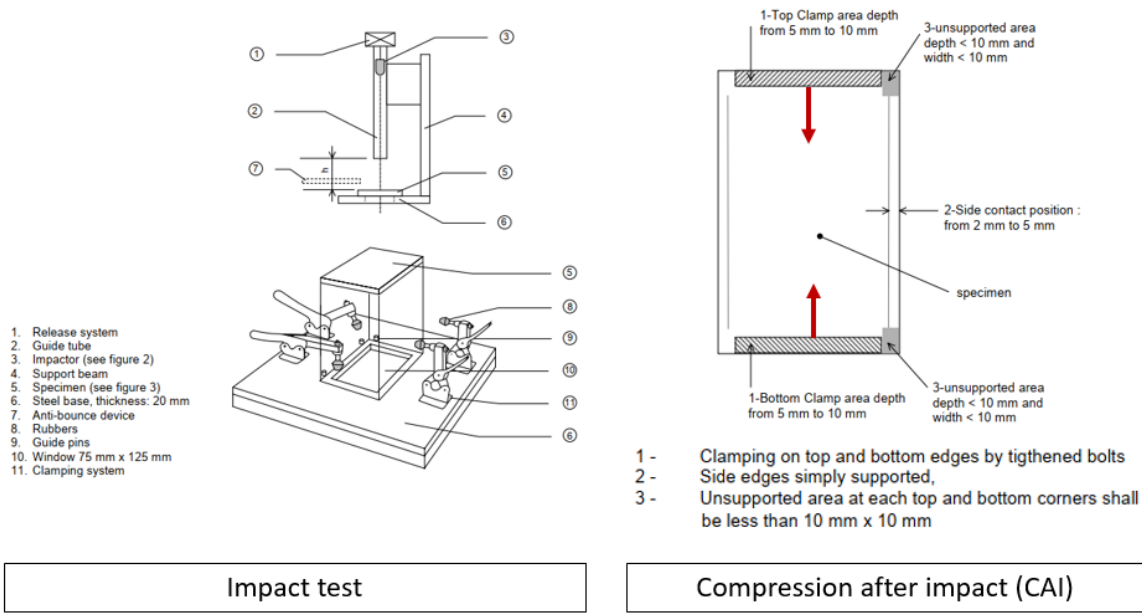


Figure 5 – Schematic representation of the BVID standard ([27])

In the BVID standard, the specimen to test is a 150x100 mm plate supported on a 125x75 mm window. The aluminum plate thickness is 2 mm, while the thickness for the composite plates is 4.2 mm. These dimensions are kept to test smart structures, but samples are equipped with piezoelectric components. The idea is to replace the compression after impact (CAI) test by the measurements of electromechanical properties to assess the integrity of the smart structure and quantify the tolerance to damage. For these measurements, the samples are removed from the impact machine and tested in free conditions to avoid dispersion due to the boundary conditions.

4.2 Samples characterization and testing

The experimental set is constituted by four different samples, which are shown in figure 6:

- Sample 1: Aluminum plate + piezoceramic (PIC155)
- Sample 2: Composite plate + piezoceramic (PIC155)
- Sample 3: Composite plate + piezocomposite (DuraAct patch)
- Sample 4: Composite plate + piezofiber (Macro Fiber Composite MFC)

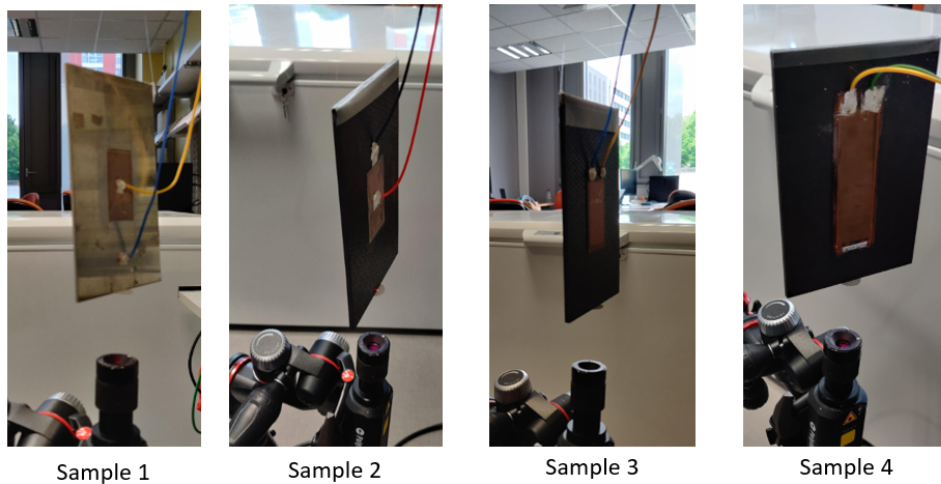


Figure 6 – Samples tested

The idea is to test the different technologies of piezoelectric actuators, illustrated in figure 7 :



Figure 7 – Technologies of piezoelectric transducers tested

The piezoceramic corresponds to a bulk piezoelectric component. The piezocomposite is the DuraAct patch made by PI, which is a bulk ceramic encapsulated between two kapton layers, allowing a prestress in compression in the ceramic. The piezofiber is similar in structure to the piezocomposite, but the bulk ceramic is replaced by fibers of PZT. These Macro Fiber Composite patches are made by Smart Material company.

The measurement of the force factor N is carried out for 3 modes, 2 symmetric flexural modes and 1 extensional mode, shown in figure 8.

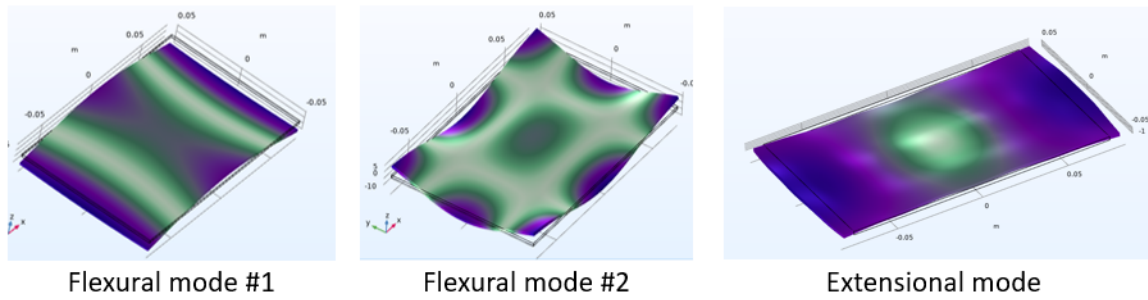


Figure 8 – Tested modes

4.2.1 Evolution of N and C_0 for the first sample

The goal is to measure the evolution of the indicators N and C_0 according to the impact energy. An iterative approach is used (figure 9). Initially, low values of impact energy are tested (0.2 J or 0.5 J) and these values are increased until a noticeable drop in the actuator performance is detected.

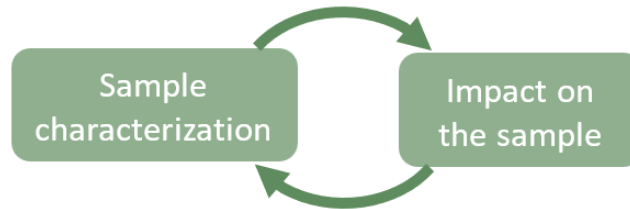


Figure 9 – Testing approach

Figures 10 and 11 show the evolution of N and C_0 for the first sample (aluminum plate + piezoceramic transducer). For this sample, a significant drop for N and C_0 is noticed after an impact of 2 J, which indicates damage in the smart structure. The measurement of C_0 is easier to repeat than the one for N . A first conclusion from these results is that there is no interest in measuring N for several modes as N decreases for all the modes. Thus, it is preferable to select only one mode which will allow an easy computation of the force factor. The measurement for extensional modes is difficult, as the laser has to be positioned in order to measure the displacement at a point located on the edge of the plate (2 or 4.2 mm thick). As a consequence of these remarks confirmed with the tests of the other samples, it is possible to conclude that the measurement of N for the first flexural mode is sufficient and recommended since it is the easiest and the most accurate way to measure the performance of the actuator.

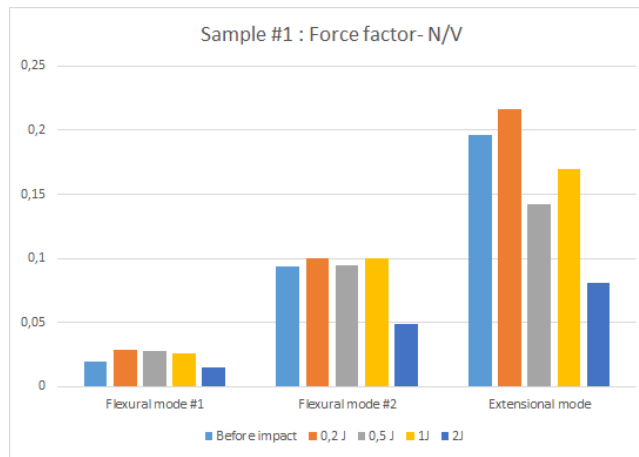


Figure 10 – Evolution of N for sample 1

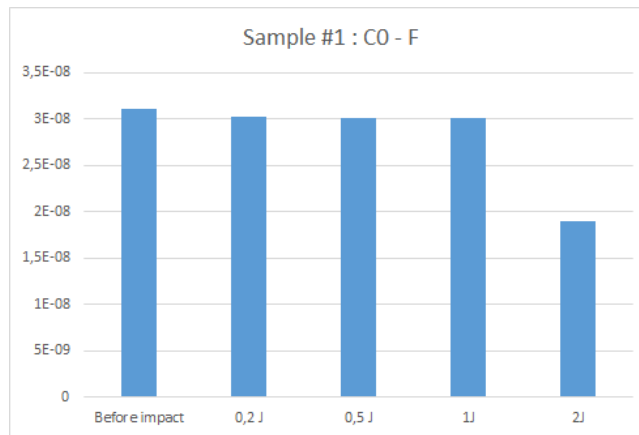


Figure 11 – Evolution of C_0 for sample 1

4.2.2 Comparison of piezoelectric technologies

Samples 2,3 and 4 are made of the same composite substrate (carbon fiber AS4 and epoxy resin 8552). This allows a comparison between the different piezoelectric technologies used.

Table 2 – Impact resistance - Samples 2,3,4

	Sample 2	Sample 3	Sample 4
Impact resistance (J)	0.5	8	10.5
ΔN	-53%	-23%	-2%
ΔC_0	-43%	-4%	-2%

Sample 2 is equipped with a bulk piezoceramic transducer. The ceramic material and the electrodes on top and bottom are brittle. This transducer is the most sensitive to impact as N and C_0 dropped for a value of impact energy of 0.5 J. For this transducer, if a cohesive crack is present, only the connected part will be operating. The loss of C_0 is proportional to the lost surface. Also, for the tests performed in this study, the ceramic is fixed to the composite substrate with an electrically conductive glue having lower mechanical properties compared to a typical epoxy glue. Therefore, it is easier to detach the transducer, which results in a lower N .

For sample 3, the piezocomposite is a piezoceramic encapsulated between two kapton layers. The fabrication process allows a prestress in compression that increase the maximum admissible stress in the ceramic. Also, the piezocomposite is fixed to the substrate with an epoxy resin with enhanced mechanical properties. For these reasons, sample 3 has a higher impact resistance and a noticeable drop of N is observed only after an 8 J impact. The electrode of the piezocomposite transducer is meshed, more resilient to impact compared to the electrodes of the piezoceramic patch. This explains

why C_0 decreased less than N .

In sample 4, the piezofiber patch has a mesh for both the electrode and the ceramic parts, increasing once more the impact resistance. The impact at 10.5 J results in the damage shown in figure 12 (a). However, despite the visible damage from the impact, the actuation function is only very slightly deteriorated as shown in figures 13 and 14. The last impact for this sample is performed at 15.7 J. As shown in figure 12 (b), the crack propagates further. The plate performances are evaluated, but the test resulted in a shortcut that prevents from retrieving any results. This is probably due to the loss of the whole piezoelectric transducer and the consequent deterioration of the contact between the plate and the PZT actuator. Considering the complete loss of electromechanical properties at 15.7 J, it is assumed that the impact resistance of the structure falls in the interval between 10.5 J and 15.7 J.

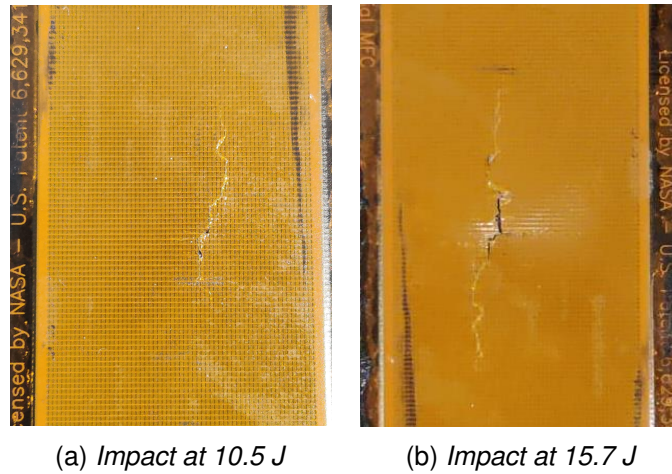


Figure 12 – Sample 4: damage to the piezoelectric transducer after impact

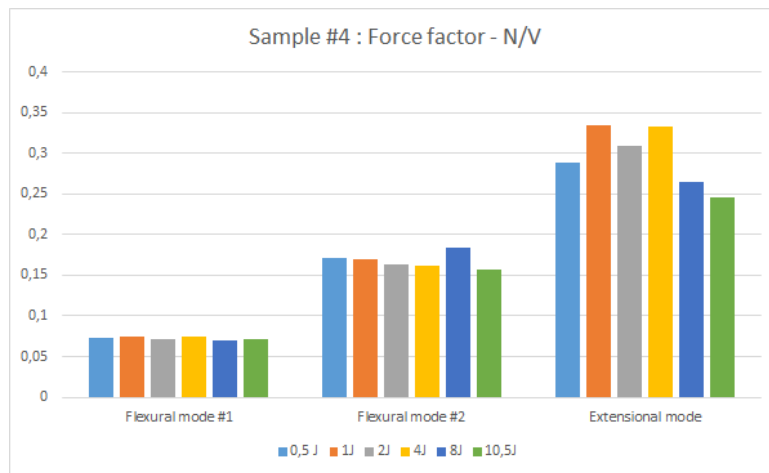


Figure 13 – Evolution of N for sample 4

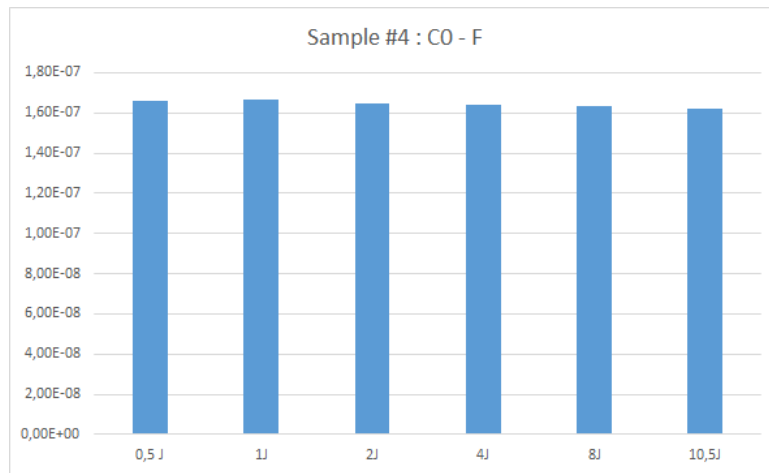


Figure 14 – Evolution of C_0 for sample 4

4.2.3 Comparison of the results with other measurement methods

Tomography A tomography was realized on sample 4 after the impact at 8 J in order to scan through the thickness of the sample. Figure 15 illustrates the image given by the tomography inside the piezofiber transducer.

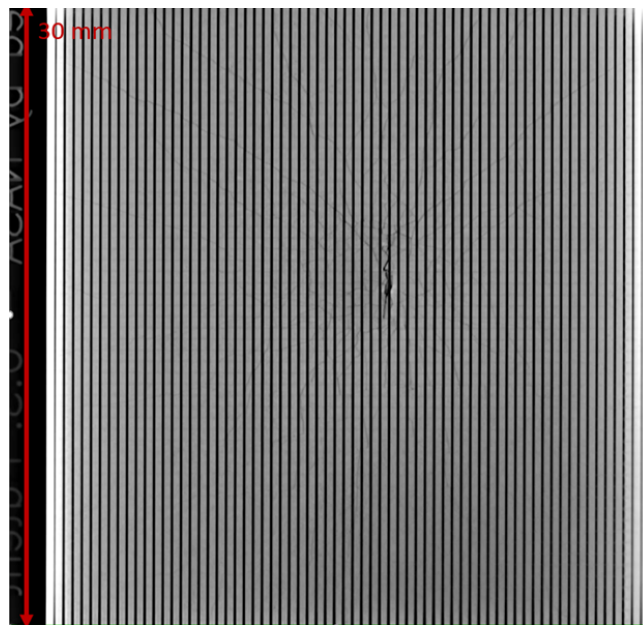


Figure 15 – Tomography of sample 4 after 8J impact

The tomography shows the cracks in the piezofiber patch. It is possible to notice that the main crack is vertical with respect to the impact location, and more cracks can be found at $\pm 45^\circ$. After the 8 J impact, the piezofiber actuator was still healthy as N and C_0 respectively dropped by only -2% and -1% . This indicates that the tomography is too pessimistic for assessing the electromechanical performances of piezoelectric actuators after an impact.

CAI test Compression after impact (CAI) tests were performed on samples 2 and 3 using a pulling machine. Figure 16 illustrates the loading curves applied to samples 2 and 3.

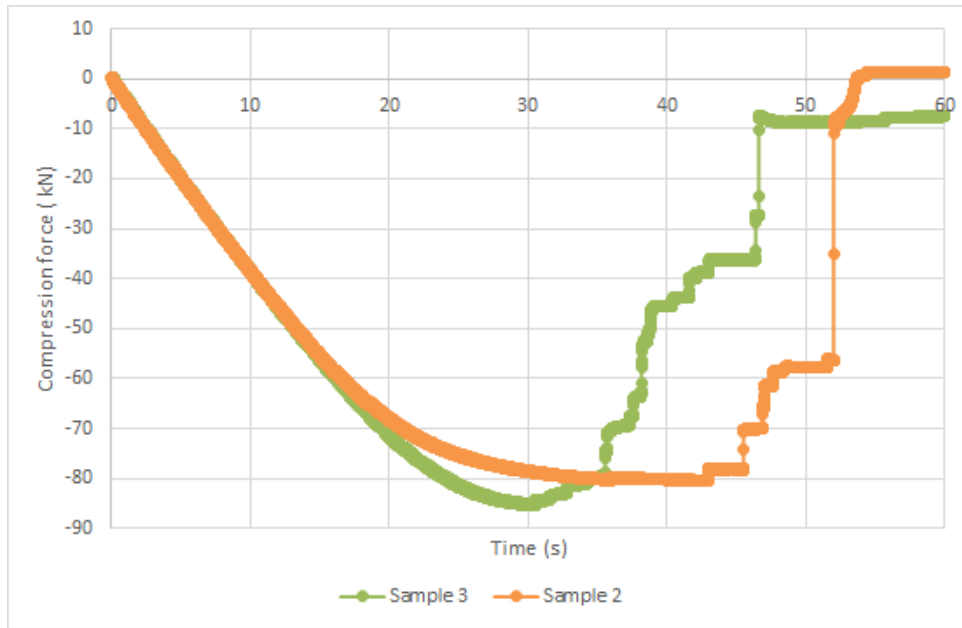


Figure 16 – Loading curves for samples 2 and sample 3

The maximum load applied on the sample corresponds to its resistance. It is possible to notice that, despite the different impact energy applied to the plates (0.5 J for sample 2, 8 J for sample 3), the resistance is close in value. Therefore, CAI test is not suitable to evaluate the functional damage on the piezoelectric transducers, as it is mostly influenced by the substrate structural health. The evaluation of the electromechanical quantities allows the detection of the changes in performances for the two specimens, which are mostly influenced by the type of piezoelectric actuator mounted on the composite substrate.

5. Conclusions

This paper aims at proposing a novel test method to measure and qualify the damage resistance of smart PZT structures to a drop-weight impact event. The method is based on the BVID method for composite materials subject to impact and adapted to smart structures. It relies on the measurements of the electromechanical characteristics of the piezoelectric transducer, the force factor N and the capacitance C_0 both in undamaged and damaged conditions. The damage is detected when a decrease of these properties occurs. Four samples considering different substrates and different actuator technologies are tested, allowing a comparison of impact resistance. A first conclusion is that the bulk piezoceramic patch is the most brittle (samples 1 and 2). The samples 3 and 4 show an improvement in the performances when adopting piezocomposites and piezofiber technologies, which are more resistant than the piezoceramic components. The piezofiber transducer has shown the highest impact resistance, but it is also more expensive if compared to the other actuators. For industrial applications, a tradeoff between the performance and the cost of application is necessary. The approach is compared with other measurement methods, the compression after impact (CAI) test and the tomography. Tomography results appear to be too pessimistic, as they indicate damage before the degradation of the actuator electromechanical performances. CAI tests are not suitable either, as the compression resistance depends mostly on the substrate structural condition and does not measure the health of the piezoelectric transducer.

In future studies, the proposed qualification test could be further validated by using a single-impact test instead of increasing the energy step by step to assess the resistance of the smart structures. The value of the impact energy would be chosen based on the results obtained in the present study.

6. Contact Author Email Address

mailto: giulia.gastaldo@isae-superaero.fr

mailto: rafik@insa-toulouse.fr

7. Acknowledgments

This project has received funding from the European Union's Horizon 2020 research and innovation program under the Marie Skłodowska-Curie grant agreement No 956703 (SURFICE Smart surface design for efficient ice protection and control).

8. Copyright Statement

The authors confirm that they, and/or their company or organization, hold copyright on all of the original material included in this paper. The authors also confirm that they have obtained permission, from the copyright holder of any third party material included in this paper, to publish it as part of their paper. The authors confirm that they give permission, or have obtained permission from the copyright holder of this paper, for the publication and distribution of this paper as part of the ICAS proceedings or as individual off-prints from the proceedings.

References

- [1] Chattopadhyay, A., Seeley, C. E., and Jha, R., "Aeroelastic tailoring using piezoelectric actuation and hybrid optimization," *Smart Materials and Structures*, vol. 8, no. 1, p. 83, 1999.
- [2] Rehman, W. U., Nawaz, H., Wang, S., Wang, X., Luo, Y., Yun, X., Iqbal, M. N., Zaheer, M. A., Azhar, I., and Elahi, H., "Trajectory based motion synchronization in a dissimilar redundant actuation system for a large civil aircraft," in *2017 29th Chinese Control And Decision Conference (CCDC)*, pp. 5010–5015, IEEE, 2017.
- [3] Grohmann, B., Maucher, C., and Jänker, P., "Actuation concepts for morphing helicopter rotor blades," in *25th International Congress of the Aeronautical sciences*, pp. 3–8, 2006.
- [4] Vos, R., "Post-buckled precompressed elements: a new class of flight control actuators enhancing morphing wing uavs," in *26th international congress of the aeronautical sciences, Anchorage, USA*, pp. 1–11, ICAS, 2008.
- [5] Budinger, M., Pommier-Budinger, V., Reysset, A., and Palanque, V., "Electromechanical resonant ice protection systems: Energetic and power considerations," *AIAA Journal*, pp. 1–13, 2021.
- [6] Staszewski, W., Boller, C., and Tomlinson, G. R., *Health monitoring of aerospace structures: smart sensor technologies and signal processing*. John Wiley & Sons, 2004.
- [7] Giurgiutiu, V., *Structural health monitoring: with piezoelectric wafer active sensors*. Elsevier.
- [8] Montalvao, D., Maia, N. M. M., and Ribeiro, A. M. R., "A review of vibration-based structural health monitoring with special emphasis on composite materials," *Shock and vibration digest*, vol. 38, no. 4, pp. 295–324, 2006.
- [9] Liu, G., Zhang, S., Jiang, W., and Cao, W., "Losses in ferroelectric materials," *Materials Science and Engineering: R: Reports*, vol. 89, pp. 1–48, 2015.
- [10] Elahi, H., Eugeni, M., and Gaudenzi, P., "Electromechanical degradation of piezoelectric patches," in *Analysis and modelling of advanced structures and smart systems*, pp. 35–44, Springer, 2018.
- [11] Friswell, M. I. and Inman, D. J., "Sensor validation for smart structures," *Journal of intelligent material systems and structures*, vol. 10, no. 12, pp. 973–982, 1999.
- [12] Kerschen, G., De Boe, P., Golinval, J.-C., and Worden, K., "Sensor validation using principal component analysis," *Smart materials and structures*, vol. 14, no. 1, p. 36, 2004.
- [13] Liang, C., "Coupled electromechanical analysis of adaptive material system-determination of actuator power consumption and system energy transfer," *Journal of Intelligent Material Systems and Structures*, vol. 5, pp. 21–20, 1994.
- [14] Sun, F., Liang, C., and Rogers, C., "Experimental modal testing using piezoceramic patches as collocated sensor-actuators," in *SEM, Spring Conference on Experimental Mechanics, Baltimore, MD*, pp. 871–879, 1994.
- [15] Giurgiutiu, V. and Craig, A. R., "Electro-mechanical (e/m) impedance method for structural health monitoring and non-destructive evaluation," 1997.
- [16] Giurgiutiu, V., Zagrai, A., and Jing Bao, J., "Piezoelectric wafer embedded active sensors for aging aircraft structural health monitoring," *Structural Health Monitoring*, vol. 1, no. 1, pp. 41–61, 2002.
- [17] Park, G., Farrar, C. R., di Scalea, F. L., and Coccia, S., "Performance assessment and validation of piezoelectric active-sensors in structural health monitoring," *Smart Materials and Structures*, vol. 15, no. 6, p. 1673, 2006.
- [18] Sun, D. and Tong, L., "Closed-loop based detection of debonding of piezoelectric actuator patches in controlled beams," *International journal of solids and structures*, vol. 40, no. 10, pp. 2449–2471, 2003.
- [19] Wang, R., Tang, E., and Yang, G., "Dynamic piezoelectric properties of pzt-5h under shock compression," *physica status solidi (a)*, vol. 216, no. 6, p. 1800859, 2019.
- [20] Wang, R., Tang, E., Yang, G., and Han, Y., "Experimental research on dynamic response of pzt-5h under impact load," *Ceramics International*, vol. 46, no. 3, pp. 2868–2876, 2020.
- [21] Elahi, H., Eugeni, M., Gaudenzi, P., Qayyum, F., Swati, R. F., and Khan, H. M., "Response of piezoelectric materials on thermomechanical shocking and electrical shocking for aerospace applications," *Microsystem Technologies*, vol. 24, no. 9, pp. 3791–3798, 2018.
- [22] Sudevan, D., Prakash, R. V., and Kamaraj, M., "Post-impact fatigue response of cfrp laminates under constant amplitude and programmed falstaff spectrum loading," *Procedia Engineering*, vol. 101, pp. 395–403, 2015.
- [23] Talreja, R. and Phan, N., "Assessment of damage tolerance approaches for composite aircraft with focus on barely visible impact damage," *Composite Structures*, vol. 219, pp. 1–7, 2019.
- [24] Abrate, S., "Modeling of impacts on composite structures," *Composite structures*, vol. 51, no. 2, pp. 129–

138, 2001.

- [25] Hawyes, V., Curtis, P., and Soutis, C., "Effect of impact damage on the compressive response of composite laminates," *Composites Part A: Applied science and manufacturing*, vol. 32, no. 9, pp. 1263–1270, 2001.
- [26] Sanchez-Saez, S., Barbero, E., Zaera, R., and Navarro, C., "Compression after impact of thin composite laminates," *Composites science and technology*, vol. 65, no. 13, pp. 1911–1919, 2005.
- [27] 1-0010, A., *Fiber reinforced plastics, determination of compression strength after impact*.
- [28] D7136/D7136M-12, A., *Standard test method for measuring the damage resistance of a fiber-reinforced polymer matrix composite to a drop-weight impact event*.
- [29] D7137/D7137M-17, A., *Standard Test Method for Compressive Residual Strength Properties of Damaged Polymer Matrix Composite Plates*.
- [30] Pommier-Budinger, V., Budinger, M., Tepylo, N., and Huang, X., "Analysis of piezoelectric ice protection systems combined with ice-phobic coatings," in *8th AIAA Atmospheric and Space Environments Conference*, p. 3442, 2016.
- [31] Pommier-Budinger, V., Budinger, M., Rouset, P., Dezitter, F., Huet, F., Wetterwald, M., and Bonaccorso, E., "Electromechanical resonant ice protection systems: initiation of fractures with piezoelectric actuators," *AIAA Journal*, vol. 56, no. 11, pp. 4400–4411, 2018.
- [32] Budinger, M., *Contribution à la conception et à la modélisation d'actionneurs piézoélectriques cylindriques à deux degrés de liberté de type rotation et translation*. PhD thesis, Institut National Polytechnique de Toulouse-INPT, 2003.